Nov 9th, 12:00 AM - 12:00 AM

Measured Geometric Imperfections for Cee, Zee, and Built-Up Cold-Formed Steel Members

X. Zhao

B. W. Schafer

Wei-Wen Yu International Specialty Conference on Cold-Formed Steel Structures
Baltimore, Maryland, U.S.A, November 9 & 10, 2016

Measured geometric imperfections for Cee, Zee, and Built-up cold-formed steel members

X. Zhao[1], B. W. Schafer[2]

Abstract

Geometric imperfections play an important role in the performance and behavior of cold-formed steel members. The objective of this paper is to present recent results from measurements of cold-formed steel members conducted by a laser scanner. The measurements provide complete and precise three-dimensional point clouds of the specimens and can be processed to determine dimensional variations as well as variations within the plates. Processing of the data can range from simple: e.g., mean lip length, to complex: e.g., modal decomposition magnitudes of the measured imperfections. Three different shapes of cold-formed steel members are selected for study: Cee, Zee, and built-up sections comprised of back-to-back Cee's. Realized dimensions of the studied cold-formed steel members are statistically explored providing mean and standard deviation and correlation data amongst the dimensions (flange width, lip length, flange-to-lip angle, etc.) can be readily performed. In addition, global (bow, camber, and twist) imperfections and cross-section Type I and Type II plate imperfections are determined from the scanned specimens. Modal imperfections decomposed into local, distortional, and global can also readily be calculated. The paper aims to demonstrate the worth of performing the three-dimensional geometric imperfection scanning and to provide useful data for simulations of cold-formed steel members. In the future it is anticipated that a systematic study of member imperfections could be used to provide definitive characterizations to help enable geometric imperfection selection in new analysis-based design approaches.

[1]Ph.D. Student, Department of Civil Engineering, Johns Hopkins University, 3400 North Charles Street, Baltimore, MD 21218; email: xzhao16@jhu.edu
[2]Professor, Department of Civil Engineering, Johns Hopkins University, 3400 North Charles Street, Baltimore, MD21218; email: schafer@jhu.edu

Introduction

The strength and stiffness of a cold-formed steel member is sensitive to geometric deviations or imperfections due to its thin-walled nature and the varying sensitivity of local, distortional, and global buckling to such imperfections. Due to this fact, imperfections in cold-formed steel members have been studied for some time. For example, Dat and Pekoz [1] measured global member out-of-straightness at the middle of the web with reference to a straight line between the ends of his specimens for his column tests. Mulligan [2] conducted similar imperfection measurements for his testing on short and long columns. Young [3] increased the imperfection measurement fidelity significantly by utilizing a single point line laser to track longitudinal imperfections along 5 cross-section points and was thus able to assess both global deviations and cross-section imperfections in detail.

Schafer and Pekoz [4] employed a set up similar in spirit to Young's using a DCDT and measured 11 lipped channel sections in detail. In addition, they categorized cross-section imperfections into Type 1 and Type 2, and compiled a database on geometric imperfections existing at that time. This work was augmented by Shifferaw et al.[5] who conducted both global and cross-section imperfections for a series of channel sections and who utlized a postion transducer on a manual linear stage to measure global imperfections for a large variety of channel sections. Even with these studies Zeinoddini and Schafer [6] concluded that the cross-section imperfection studies available to date are not of high enough fidelity (dense enough in their imperfection information) for many advanced numerical simulations and improved measurements are needed.

Zhao et al. [7] developed a 3D laser measurement platform which can provide full-field measurement point clouds of target specimens placed on the platform. Extracted geometry information from measurement point clouds allows traditional cross-section imperfections to be better estimated, such as Type 1 and Type 2 imperfections, but also afford opportunities to measure other imperfection quantities and even dimensional quantities. Most past imperfection measurements have focused on lipped and unlipped channel sections; few studies of geometric imperfections are carried out on other cold-formed steel shapes.

This paper demonstrates the application of the laser measurement platform developed by Zhao and Schafer [8]; including determination of dimensional variations, as well as global and cross-section imperfections for Zee, Cee, and built-up sections. The second section of this paper provides background on the laser measurement platform and the measurement schemes employed.

Dimensions of the three different shapes studied are collected and statistically analyzed in the following section. Next, imperfection measurements and related statistical analysis are presented, followed by discussion and conclusions.

Background of Laser Measurement

An imperfection measurement rig, Figure 1, was constructed in the Thin-Walled Structures Laboratory at Johns Hopkins University. The objective of the imperfection measurement rig is to achieve reasonably high-throughput and high-accuracy representations of the three-dimensional geometry of as-manufactured members, for example, cold-formed steel members in this paper. The imperfection rig is designed to measure a specimen of at least 10 in (250 mm) in width or depth and 8 feet (2400 mm) long, which in turn determined the scanning area. The imperfection measurement rig contains three major components: laser scanner, rotary stage, and linear stage.

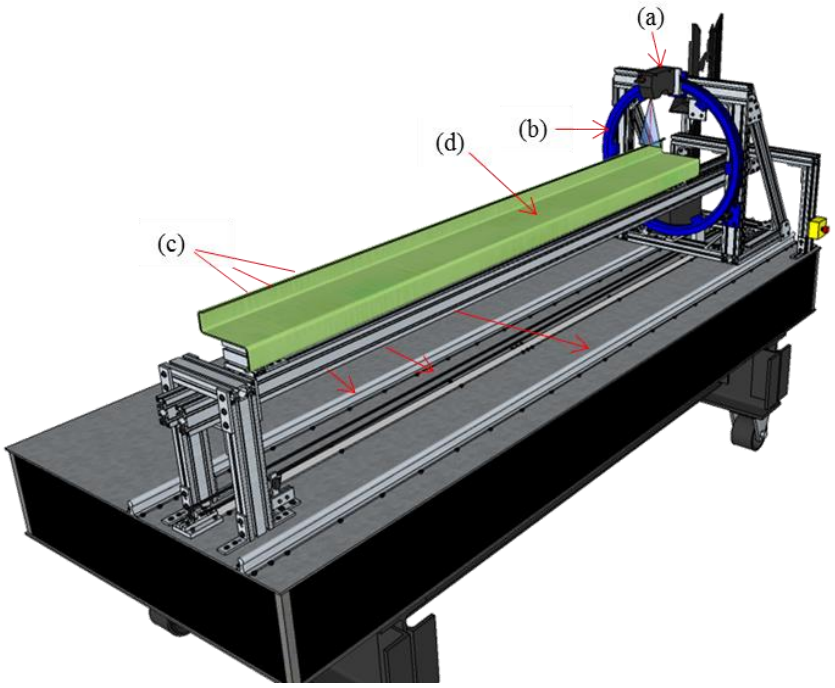

Figure 1 Laser-Based Imperfection Measurement Platform: (a) Laser Scanner; (b). Large Rotary Stage; (c). Linear Motion System; (d). Zee-shaped Specimen

The laser scanner is a 2D line laser which can generate 800 points per reading, covering a width of up to 9.5 in (240 mm). The laser is installed on a rotary stage, the diameter of which is 25 in (635 mm). This allows the laser to scan different segments of a target specimen while the stage rotates. The linear motion system drives the rotary ring and positions the laser along the specimen. Full-field geometric information of a target specimen can be achieved by scanning the specimen at multiple angles of view and registering the individual scans into the same final global coordinate system (Figure 2). In general, the number of scan angles depends on the complexity of the geometry in order to achieve the desired resolution of scanning segments. In the work conducted here, a Zee shape required seven different angles for building up the measurement, while a Cee shape required five different angles, and a built-up shape required nine different angles to develop the desired resolution. Further documentation of the imperfection measurement rig is available in Zhao, et al. [7].

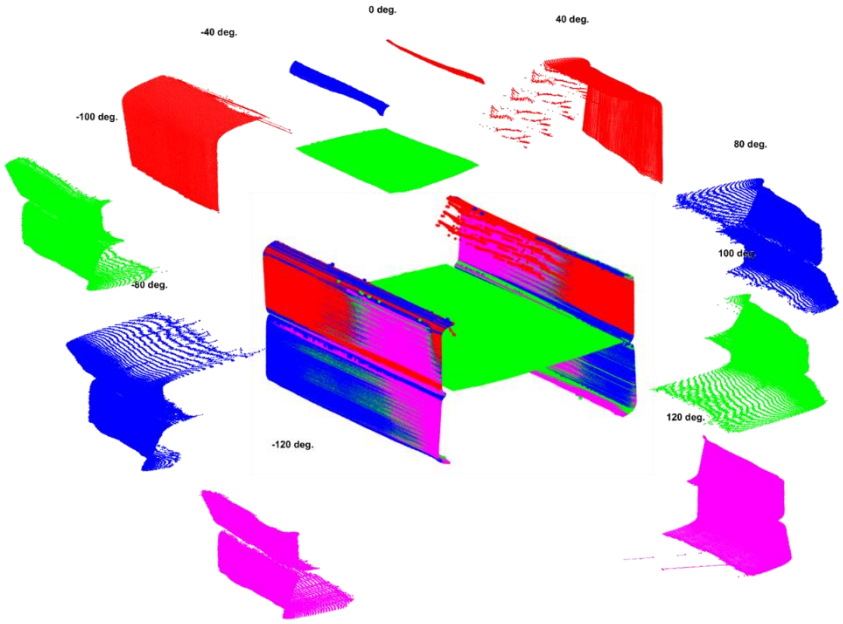

Figure 2 Example of Nine Different Scans Used to Develop Built-up Cee

A series of steps are applied to the scanned segments to develop a full model. The scanned segments are first globally registered and colored based on deviation from nominally expected dimensions as shown in Figure 3. The reconstructed 3D models are categorized based on its geometric characteristics, i.e. corners, lips, flanges, and web [9]. Results from this step can be applied into studies on

dimensions, imperfection estimations, or even used as the true geometry in shell finite element modeling. This paper mainly discusses the first two applications, see Zhao, et al. [9] for an example of the last application.

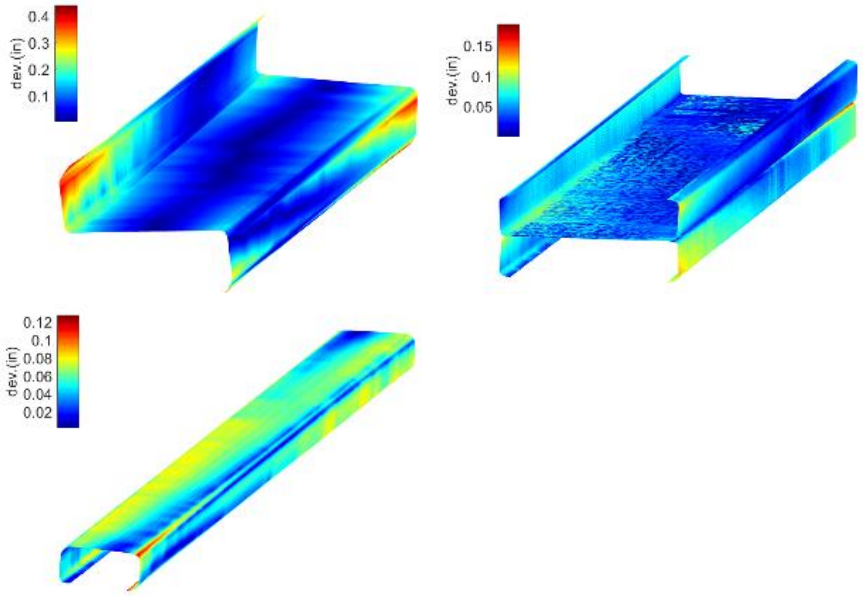

Figure 3 Example 3D Reconstructed Models from Laser Measurement Platform; (a) Zee; (b) Built-up Cees; (c) Cee

Analysis of Member Dimensions from Laser Scanner Data

Dimension Definition

One important application from laser measurement point clouds is the calculation of cross-section dimensions. Dimensional variation, which can be considered as a primary imperfection, leads to variation in section properties, contributing to variation of strength and stiffness of a structural member. However, due to the constraints of conventional dimensional measurement tools, minimal statistical data exists on cold-formed steel cross-section variation. Thus, the laser measurement point clouds potentially fill in this gap. Dimensions of three shapes of studs have been estimated from reconstructed laser measurement models. Dimensional quantities are in Figure 4-6. Radii are estimated from corners. Best-fit linear segments are fit to other regions intersections of which are used for estimating out-to-out dimensions.

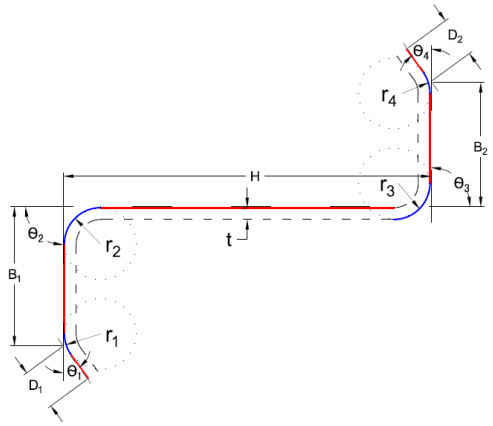

Figure 4 Dimension Definition for Zee Shape

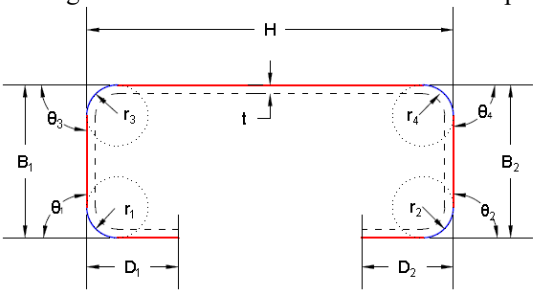

Figure 5 Dimension Definition for Cee Shape

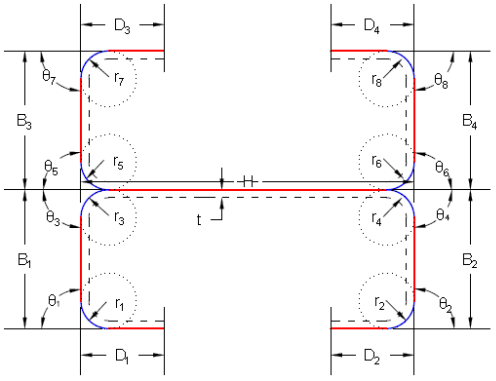

Figure 6 Dimension Definition for Built-Up Cee Shape

Dimension summary from measurements

The study conducted herein includes 19 nominally identical Zees, 8 Cees, and 8 members built-up from Cees. The Zees members are all 4 ft (1219 mm) long and 7 in. (178 mm) deep (additional dimensional details in Table 1). The Cees are of two types, i.e., four 362S162-68 specimens and four 600S137-54 specimens (AISI S200-12 nomenclature). Similar to the Cees, the built-up members contain two different types, eight 362S162-68 specimens comprising four built-up members, and eight 600S137-54 specimens comprising an additional four built-up members. Both the Cees and built-up Cees are 6 ft (1829 mm) long.

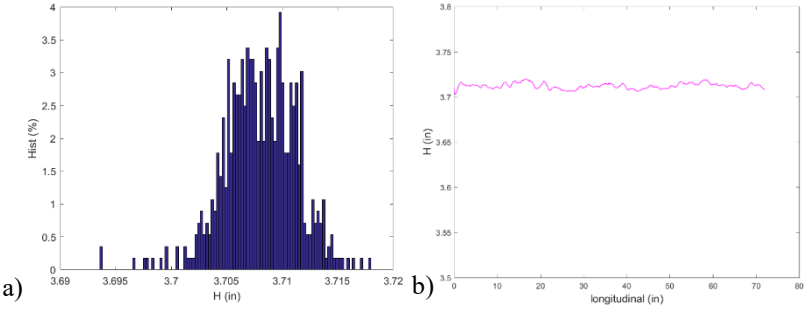

Figure 7 Typical Dimension Measurement of a Scanned Cee Specimen; (a) Histogram of Web Heights; (b) Typical Web Height Longitudinal Variation

Typical dimensions derived from the laser scanned point clouds are provided in Figure 7 for a single specimen. Statistical summaries including the 5%, 10% and 50% CDF values for the dimensions as well as the mean and standard deviation of the dimensions are provided with respect to the Zee, Cee, and built-up members in Table 1 - 3. Comparisons are also provided to the nominal specified dimensions in the Table.

As expected, variation in the web depth, compared to all other dimensional quantities, are minimal in general. Corner radii, in general, differ greatly from specified dimensions. However, corners adjacent to the web generally have better manufacturing control and the difference with nominal dimensions are smaller than those adjacent to the lips. Angles between elements, particularly the flange and lip, also have large variations. The statistics supplied here can be used to develop cross-sections with a certain probability of occurrence, compare against quality control standards, or form the basis for fundamental reliability studies.

Table 1 Statistical dimension summary from laser measurements of Zee shape studs

Dimension		H (in)	B_1 (in)	B_2 (in)	D_1 (in)	D_2 (in)	r_1 (in)	r_2 (in)	r_3 (in)	r_4 (in)	θ_1 (°)	θ_2 (°)	θ_3 (°)	θ_4 (°)
Laser	5%	6.94	2.20	2.24	0.64	0.76	0.47	0.37	0.29	0.42	40.7	86.2	86.3	41.7
	10%	6.95	2.21	2.26	0.68	0.76	0.49	0.38	0.30	0.43	41.0	87.1	87.1	41.8
	50%	6.96	2.23	2.28	0.73	0.78	0.53	0.40	0.32	0.45	41.8	89.0	88.5	42.4
	Mean	6.96	2.23	2.29	0.73	0.78	0.53	0.39	0.33	0.45	41.9	88.8	88.5	42.4
	Std	0.05	0.04	0.05	0.07	0.02	0.03	0.02	0.04	0.02	1.9	2.6	1.3	1.0
Nominal		7.00	2.25	2.25	0.77	0.77	0.37	0.37	0.37	0.37	48	90	90	48
L. vs. N. (%)		-0.6	-1.1	1.92	-5.3	1.18	41.1	6.02	-11	21.5	-12	-1.3	-1.7	-11

Table 2a Statistical dimension summary of Cee shape section [Stud: 362S162-68]

Dimension		H (in)	B_1 (in)	B_2 (in)	D_1 (in)	D_2 (in)	r_1 (in)	r_2 (in)	r_3 (in)	r_4 (in)	θ_1 (°)	θ_2 (°)	θ_3 (°)	θ_4 (°)
Laser	5%	3.71	1.59	1.60	0.46	0.45	0.27	0.26	0.29	0.32	74.5	76.5	91.3	91.1
	10%	3.71	1.60	1.60	0.47	0.45	0.28	0.26	0.30	0.33	74.7	76.3	91.6	91.3
	50%	3.72	1.61	1.69	0.53	0.48	0.32	0.28	0.32	0.35	75.7	86.1	92.0	92.4
	Mean	3.72	1.63	1.67	0.52	0.49	0.31	0.29	0.33	0.35	78.1	84.9	92.3	92.5
	Std	0.01	0.04	0.04	0.03	0.03	0.02	0.03	0.04	0.02	4.60	5.27	0.93	1.03
Nominal		3.63	1.63	1.63	0.50	0.50	0.18	0.18	0.18	0.18	90	90	90	90
L. vs. N. (%)		2.47	0.00	2.45	4.00	-2.0	72.2	61.1	83.3	94.4	-13	-5.7	2.56	2.7

Table 2b Statistical dimension summary of Cee shape section [Stud: 600S137-54]

Dimension		H (in)	B_1 (in)	B_2 (in)	D_1 (in)	D_2 (in)	r_1 (in)	r_2 (in)	r_3 (in)	r_4 (in)	θ_1 (°)	θ_2 (°)	θ_3 (°)	θ_4 (°)
Laser	5%	5.99	1.27	1.27	0.37	0.36	0.17	0.17	0.12	0.12	76.5	76.7	86.8	86.9
	10%	6.00	1.27	1.27	0.38	0.37	0.17	0.17	0.13	0.13	76.8	77.0	87.4	87.4

Table 2b (Continued)

Laser	50%	6.00	1.30	1.30	0.40	0.39	0.18	0.18	0.14	0.14	78.7	79.2	87.8	88.0
	Mean	6.00	1.30	1.30	0.40	0.39	0.18	0.18	0.14	0.14	79.0	79.1	87.8	88.0
	Std	0.01	0.02	0.02	0.02	0.02	0.01	0.01	0.01	0.01	1.80	1.50	0.67	0.73
Nominal		6.00	1.38	1.38	0.38	0.38	0.14	0.14	0.14	0.14	90	90	90	90
L. vs. N. (%)		0.00	-5.8	-5.8	5.3	2.6	28.6	28.6	0.00	0.00	-12	-12	-2.4	-2.2

Table 3a Statistical dimension summary of Built-up Cee section [Stud: 362S162-68]

Dimension (Lower)		H (in)	B_1 (in)	B_2 (in)	D_1 (in)	D_2 (in)	r_1 (in)	r_2 (in)	r_3 (in)	r_4 (in)	θ_1 (°)	θ_2 (°)	θ_3 (°)	θ_4 (°)
Laser	5%	3.69	1.60	1.59	0.47	0.45	0.25	0.26	0.32	0.30	73.7	75.2	91.5	90.8
	10%	3.70	1.60	1.60	0.48	0.46	0.26	0.27	0.32	0.31	74.0	75.5	91.7	90.9
	50%	3.71	1.62	1.71	0.52	0.49	0.31	0.29	0.35	0.35	76.0	87.5	92.5	92.5
	Mean	3.71	1.63	1.68	0.51	0.49	0.30	0.29	0.36	0.34	77.5	85.2	92.6	92.4
	Std	0.01	0.03	0.05	0.02	0.02	0.03	0.02	0.03	0.03	3.87	5.74	0.74	0.96
Nominal		3.63	1.63	1.63	0.50	0.50	0.18	0.18	0.18	0.18	90	90	90	90
L. vs. N. (%)		2.20	0.0	3.1	2.0	-2.0	67.7	61.1	100	88.9	-14	-5.3	2.88	2.67
Dimension (Upper)		H (in)	B_3 (in)	B_4 (in)	D_3 (in)	D_4 (in)	r_5 (in)	r_6 (in)	r_7 (in)	r_8 (in)	θ_5 (°)	θ_6 (°)	θ_7 (°)	θ_8 (°)
Laser	5%	3.69	1.61	1.59	0.47	0.48	0.29	0.31	0.22	0.23	90.9	90.9	75.3	74.5
	10%	3.70	1.61	1.60	0.47	0.49	0.30	0.32	0.23	0.23	91.2	91.4	75.7	75.1
	50%	3.71	1.66	1.63	0.51	0.52	0.36	0.35	0.28	0.28	92.5	92.6	80.5	79.6
	Mean	3.71	1.66	1.65	0.51	0.52	0.35	0.35	0.28	0.28	92.4	92.4	82.3	82.6
	Std	0.01	0.03	0.05	0.03	0.03	0.03	0.03	0.04	0.03	0.85	0.60	5.64	6.73
Nominal		3.63	1.63	1.63	0.50	0.50	0.18	0.18	0.18	0.18	90	90	90	90
L. vs. N. (%)		2.20	1.84	1.23	2.0	4.0	94.4	94.4	55.6	55.6	2.67	2.67	-8.6	-8.2

Table 3b Statistical dimension summary of Built-up Cee section [Stud: 600S137-54]

Dimension (Lower)		H (in)	B_1 (in)	B_2 (in)	D_1 (in)	D_2 (in)	r_1 (in)	r_2 (in)	r_3 (in)	r_4 (in)	θ_1 (°)	θ_2 (°)	θ_3 (°)	θ_4 (°)
Laser	5%	5.96	1.27	1.27	0.37	0.35	0.17	0.17	0.10	0.11	77.5	76.6	87.5	87.6
	10%	5.96	1.28	1.27	0.38	0.36	0.18	0.17	0.11	0.12	78.0	77.1	88.0	88.0
	50%	5.97	1.33	1.30	0.40	0.38	0.20	0.20	0.14	0.14	83.3	80.0	88.5	88.5
	Mean	5.97	1.33	1.30	0.40	0.38	0.20	0.20	0.14	0.14	82.4	80.0	88.5	88.6
	Std	0.01	0.02	0.02	0.02	0.02	0.01	0.02	0.02	0.02	2.54	1.68	0.81	0.69
Nominal		6.00	1.38	1.38	0.38	0.38	0.14	0.14	0.14	0.14	90	90	90	90
L. vs. N. (%)		-0.5	-3.6	-5.8	5.26	0.00	42.8	42.8	0.00	0.00	-8.4	-11	-1.7	-1.6
Dimension (Upper)		H (in)	B_3 (in)	B_4 (in)	D_3 (in)	D_4 (in)	r_5 (in)	r_6 (in)	r_7 (in)	r_8 (in)	θ_5 (°)	θ_6 (°)	θ_7 (°)	θ_8 (°)
Laser	5%	5.96	1.28	1.28	0.36	0.29	0.12	0.12	0.15	0.17	78.0	87.3	78.0	77.8
	10%	5.96	1.29	1.28	0.37	0.31	0.13	0.12	0.16	0.17	79.3	87.4	78.4	78.6
	50%	5.97	1.34	1.30	0.41	0.40	0.14	0.14	0.17	0.19	86.8	87.8	82.3	81.1
	Mean	5.97	1.33	1.31	0.41	0.38	0.14	0.14	0.17	0.19	85.1	88.0	82.1	81.0
	Std	0.01	0.03	0.02	0.03	0.05	0.01	0.01	0.01	0.01	3.78	0.56	2.52	2.21
Nominal		6.00	1.38	1.38	0.38	0.38	0.14	0.14	0.14	0.14	90	90	90	90
L. vs. N. (%)		-0.5	-3.6	-5.0	-7.9	0.00	0.00	0.00	21.4	35.7	-5.4	-2.2	-8.8	-10

Analysis of Imperfections from Laser Scanner Data

Imperfection Definition

Geometric imperfections can be automatically identified from the measurement point clouds, e.g. Figure 3, for different member geometries. In this paper, three member types are studied following conventional imperfection definitions, i.e.: [4]. Figure 8 through Figure 10 depict the 3 global imperfections related to bow, camber and twist, and the 2 cross-sectional imperfections related to Type 1 (d_1) and Type 2 (d_2) for the Cee, built-up Cee, and Zee sections respectively.

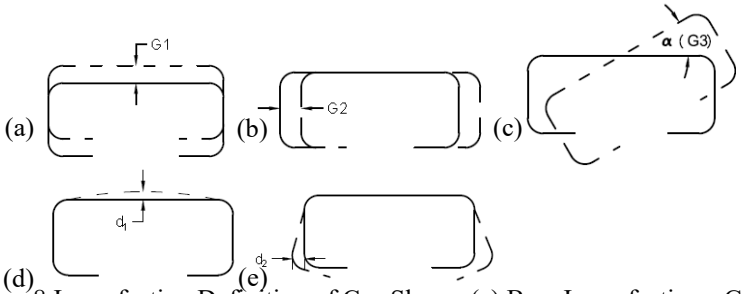

Figure 8 Imperfection Definition of Cee Shape; (a) Bow Imperfection - G1; (b) Camber Imperfection - G2; (c) Twist Imperfection - G3; (d) Type 1 Imperfection - d_1; (e) Type 2 Imperfection - d_2

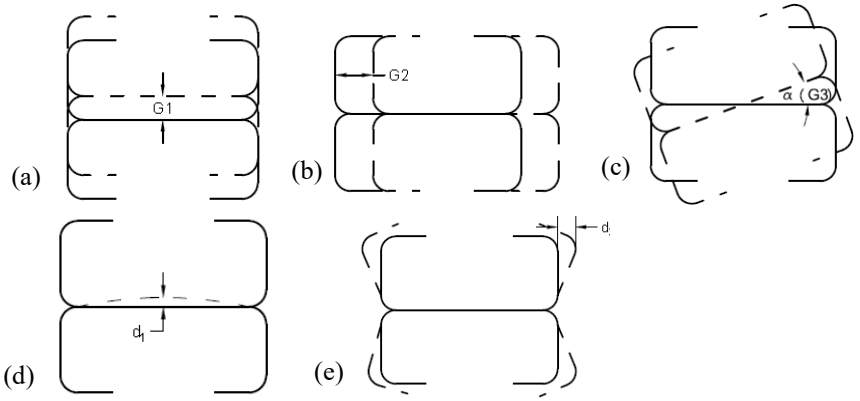

Figure 9 Imperfection Definition of Built-up Cee Section; (a) Bow Imperfection - G1; (b) Camber Imperfection - G2; (c) Twist Imperfection - G3; (d) Type 1 Imperfection - d_1; (e) Type 2 Imperfection - d_2

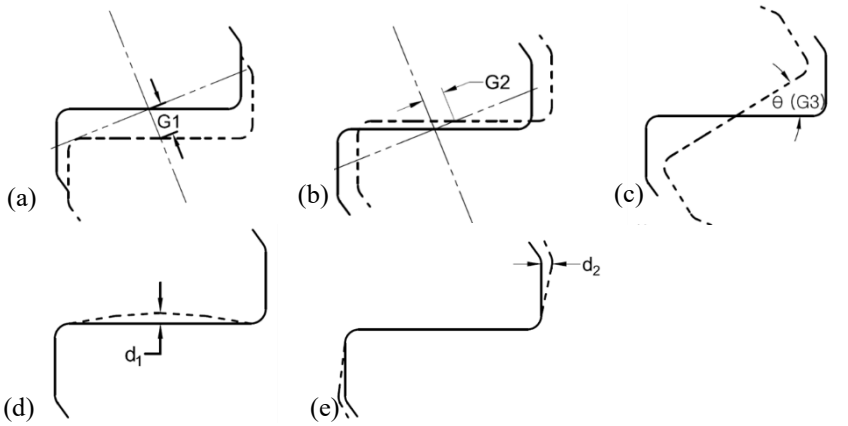

Figure 10 Imperfection Definition of Zee Shape; (a) Bow Imperfection - G1; (b) Camber Imperfection - G2; (c) Twist Imperfection - G3; (d) Type 1 Imperfection - d_1; (e) Type 2 Imperfection - d_2

The imperfection magnitudes are calculated from the reconstructed three-dimensional point clouds from the laser scanner (i.e. Figure 3). Bow (G1) and camber (G2) imperfections are established by finding the centroid of each measured cross- section and comparing to the nominal cross-section centroid. It is always assumed that centroids at the ends' of the sections coincide with those of the nominally perfect specimens. The maximum values found from the comparisons are denoted as extreme imperfections of bow and camber respectively (one per each measured specimen – this statistic is collected because historically this value was often recorded). A mid-span cross-section is used to find the angle of twist of the entire specimen. The angle of twist is defined as the difference between the two ends, and is the extreme G3 imperfection. Cross-section imperfection, Type 1 magnitude (d_1) is constructed by fitting a best-fit line to the ends of the web flat region and taking the maximum perpendicular deviation from that line. Type 2 magnitude (d_2) is constructed from every cross-section by projecting an ideal flange 90° from the web flat and finding the perpendicular distance from this ideal flange to the measured flange.

Imperfection Measurement Summary

A typical realization for G1, G2, G3, d_1, and d_2 imperfections along the length of a specimen are provided in Figure 11. The results are consistent across most specimens and suggest first buckling mode shapes for G1 and G2 are generally consistent with measured imperfections. Twist (G3) and cross-section imperfections are more complex and analysis in the frequency domain can be useful [10].

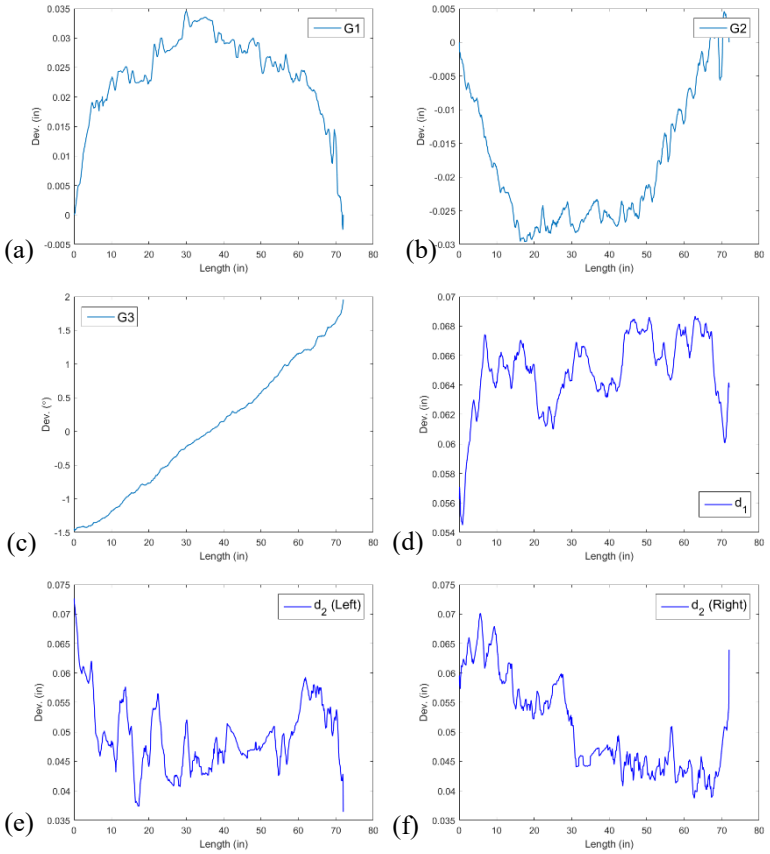

Figure 11 Typical Imperfection Findings towards a target sample; (a) Bow Imperfection - G1; (b) Camber Imperfection - G2; (c) Twist Imperfection - G3; (d) Type 1 Imperfection - d_1; (e) Type 2 Imperfection - d_2 of Left Flange; (f) Type 2 Imperfection - d_2 of Right Flange.

Although complete CDFs can be constructed, only the mean and standard deviation of the maximum measured imperfections are provided in Table 4. In addition, the 50% CDF values from past studies (Zeinoddini and Schafer 2014) and the maximum tolerances from ASTM C955 are provided for reference. The measured imperfections indicate that current tolerances can be challenging to meet particularly for camber (G2), twist (G3), and cross-section/element out-of-straightness (d_2). Also, imperfections for the studied Zees are considerably larger than the typical imperfections summarized through past data (listed as Zeinoddini in Table 4).

Table 4 Statistical summary of maximum geometric imperfections

		Type1 d_1/t	Type2 d_{2L}/t	Type2 d_{2R}/t	Type1 d_1/t	Type2 d_{2L}/t	Type2 d_{2R}/t	G1 L/δ	G2 L/δ	G3 °/ft
	mean	1.086	1.073	1.010	1.238	1.19	1.327	3772	1705	0.2
BUC[a]	std.dev.	0.441	0.299	0.283	0.434	0.428	0.342	2356	538	0.1
Cee	mean	1.05	1.471	1.360				1754	2806	0.2
	std.dev.	0.046	0.552	0.581				952	745	0.2
Zee	mean	0.68	1.78	3.37				1000	372	1.7
	std.dev.	0.23	0.5	1.78				2087	857	0.3
	50%[b]	0.34	0.94	0.94	0.34	0.94	0.94	2242	3477	0.1
	C955[c]		1.05	1.05		1.05	1.05	960	960	0.1

Notes:

a. BUC indicates built-up Cee shape

b. statistical summary from measurements on lipped channels [10]

c. reference tolerances from ASTM C955 for Cees, d_2 tolerance is $\pm 1.05t$; G1 (bow) and G2 (camber) are L/960; G3 is 1/32 in./ft of a specimen.

Discussion

Technology related to the ability to scan 3D objects and create accurate point clouds of the resulting object is growing quickly. The potential of such information is vast, particularly for imperfection sensitive objects such as thin-walled cold-formed steel members. This paper provides an introduction to the possibilities of what may be realized through such information based on measurements of industry standard profiles using a laser scanner. Additional examples are discussed in Zhao et al. [9]. Information on using photogrammetry for similar measurements in cold-formed steel are also available [11] . In addition, the potential to use the scanner information in reliability studies [12] or to improve simulated imperfections [10] also significant. The first author is currently completing her Ph.D. dissertation on this topic with a dissertation expected in the Summer of 2016.

Conclusions

High-throughput high accuracy laser-based measurements may be performed to develop accurate 3D point clouds of cold-formed steel cross-sections. Scans on Cees, Zees, and built-up Cee shapes are completed to demonstrate the potential of the recorded data. With tens of thousands of points per specimen it is possible to provide highly accurate dimensions as well as the statistics of how dimensions vary along the member length. In addition, it is readily possible to synthesize the data to point estimates at desired statistical levels for key imperfection quantities such as bow, camber, twist, plate flatness, and element out-of-straightness. Together these provide powerful tools in potential quality control and quality assurance measures. The laser scanning also affords a number of additional possibilities in simulation and reliability studies that can significantly aid in our understanding of cold-formed steel members.

Acknowledgements

The authors would like to thank Dave Fratamico for his help in built-up members scanning. This work was partially funded by the National Science Foundation (NSF), Grant 1235196. Any opinions, findings, conclusions, or recommendations stated are those of author(s) and do not necessarily reflect the views of the National Science Foundation.

References

[1] D. T. Dat and T. P. Pekoz, "Report: The strength of cold-formed steel columns," Cornell University, Ithaca, NY1980.

[2] G. P. Mulligan, "The influence of local buckling on the structural behavior of singly symmetric cold-formed steel columns," Ph.D., Cornell University, Ithaca, NY, 1983.

[3] B. Young, Rasmussen, K.J.R., "Measurement techniques in the testing of thin-walled structural members.," *Experimental Mechanics,* vol. 43, pp. 32-38, 2003.

[4] B. W. Schafer and T. Pekoz, "Computational modeling of cold-formed steel: characterizing geometric imperfections and residual stresses," *Journal of Constructional Steel Research,* vol. 47, pp. 193-210, 1998.

[5] L. C. M. Vieira JR., Y. Shifferaw, and B. W. Schafer, "Experiments on sheathed cold-formed steel studs in compression.," *Journal of Constructional Steel Research,* vol. 67, pp. 1554-1566, 2011.

[6] V. Zeinoddini and B. W. Schafer, "Global imperfections and dimensional variations in cold-formed steel members," *International Journal of Structural Stability and Dynamics,* vol. 11, pp. 829-854, 2011.

[7] X. Zhao, M. Tootkaboni, and B. W. Schafer, "Development of a Laser-Based Geometric Imperfection Measurement Platform with Application to Cold-Formed Steel Construction," *Experimental Mechanics,* vol. 55, pp. 1779-1790, 2015.

[8] X. Zhao and B. W. Schafer, "Laser scanning to develop three-dimensional fields for the precise geometry of cold-formed steel members," in *Recent Research and Developments in Cold-Formed Steel Design and Construction*, St. Louis, MO, 2014, pp. 97-114.

[9] X. Zhao, M. Tootkaboni, and B. W. Schafer, "Laser-based Cross-Section Measurement of Cold-Formed Steel Members: Model Reconstruction and Application," *Thin-Walled Structures,* 2016.

[10] V. M. Zeinoddini and B. W. Schafer, "Simulation of geometric imperfections in cold-formed steel members using spectral representation approach," *Thin-Walled Structures,* vol. 60, pp. 105-117, 2012.

[11] L. E. McAnallen, D. A. Padilla-Llano, X. Zhao, C. D. Moen, B. W. Schafer, and M. R. Eatherton, "Initial geometric imperfection measurement and characterization of cold-formed steel c-section structural members with 3D non-contact measurement techniques," in *Proceedings of the Annual Stability Conference* Toronto, Canada, 2014.

[12] A. W. Fischer and B. W. Schafer, "Impact of fabrication tolerances on cold-formed steel section properties, stability, and strength," in *SSRC*, Orlando, FL, 2016.